Model based feedback control of resistive wall modes using external coils

J.M. Hanson[1,2], O. Katsuro-Hopkins[1], J. Bialek[1], H. Reimerdes[1], Y. In[3], M.J. Lanctot[1], G.A. Navratil[1], M. Okabayashi[4], and E.J. Strait[5]

[1]*Columbia University, 500 W. 120th Street, New York, NY 10027, USA*
[2]*Oak Ridge Institute for Science & Education, PO Box 117, Oak Ridge, TN 37831, USA*
[3]*FAR-TECH, Inc., 3550 General Atomics Court, San Diego, CA 92121, USA*
[4]*Princeton Plasma Physics Laboratory, PO Box 451, Princeton, NJ 08543-0451, USA*
[5]*General Atomics, PO Box 85608, San Diego, CA 92186, USA*

A promising avenue toward achieving stable tokamak operation above the no wall beta limit for the resistive wall mode (RWM) involves the use of magnetic feedback to detect and stabilize the mode. Although feedback stabilization experiments using classical control algorithms have met with some success, model-based feedback control algorithms can improve feedback performance when coils external to the vacuum vessel are used. A linear-quadratic-Gaussian (LQG) controller has been designed based on a three-dimensional VALEN [J. Bialek, *et al.,* Phys. Plasmas **8**, 2170 (2001)] model for the DIII-D vacuum vessel wall and coil sets. Stability calculations using only external coils indicate that the LQG controller can stabilize the RWM at an open-loop growth rate for which proportional gain feedback fails.

1. Introduction

The control or avoidance of long-wavelength MHD instabilities that arise at high pressures in tokamak plasmas will likely be important for the success of steady-state, high fusion gain scenarios in ITER [1] and for future tokamak devices that seek to maximize fusion output. One such instability, the n=1 RWM, has been successfully controlled using feedback with magnetic coils [2–4].

The optimization of feedback algorithms and hardware for RWM control is ongoing. Improved performance has been attained using control coils that are internal to the vacuum vessel [5], and a set of internal coils has been proposed for ITER. However, maintaining in-vessel coil arrays may prove to be impractical for future burning plasma devices.

Model-based feedback algorithms have the potential to improve feedback with external coils beyond what is achievable with proportional gain control. Kalman filtering has been used in experiments to improve RWM feedback in the presence of noise [6–8], and simulations of RWM feedback in ITER with the planned external error-field correction coils indicate that performance can be improved using a linear-quadratic-Gaussian (LQG) control algorithm that incorporates a three-dimensional VALEN [9] model for the control and sensor coils, vacuum vessel wall, and plasma stability [10]. In this paper, we describe an LQG RWM controller that is designed for feedback with DIII-D's external coils, using the prescription of Katsuro-Hopkins *et al.* [10].

2. Current-driven resistive wall mode behaviour in DIII-D

In recent years, low-beta, current-driven RWMs have become the standard target for feedback experiments in DIII-D due to their ease of reproducibility [11]. DIII-D discharge 133021 provides an example of current-driven RWM activity. In this shot, the plasma current was ramped at a rate of ~1 MA/s using transformer action, leading to a broad current density profile. DIII-D's external non-axisymmetric coils were used to provide error field correction. Figure 1 shows the time evolutions of q_{95} and the amplitude and toroidal phase of the perturbed n=1 poloidal magnetic field at the outboard midplane. As q_{95} approaches 4.0, a toroidally rotating instability is observed in the magnetics. An initial phase of exponential growth at a rate of ~0.4 ms^{-1} is observed just after t = 460 ms. During the next 25 ms, the growth of the mode slows, and the amplitude saturates near the time t = 500 ms. Instabilities generated in this manner have been shown to respond to magnetic feedback [11].

An equilibrium for shot 133021 was obtained at time t = 445 ms, just before the instability is observed to grow. A stability analysis of this equilibrium performed with the DCON [12] code shows that it is unstable to an n=1, external mode. A VALEN eigenvalue calculation yields an open-loop growth rate of 0.233 ms^{-1} for the n=1 instability in the presence of a three-dimensional, resistive model for the DIII-D vacuum vessel wall.

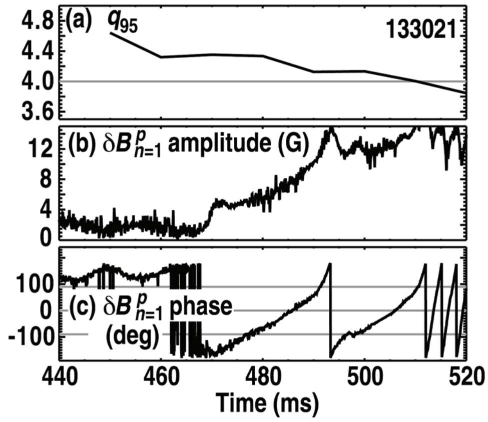

Fig 1. Time evolutions of (a) q_{95} and (b) the amplitude and (c) toroidal phase of the perturbed n=1 poloidal field.

3. LQG controller design

In contrast to classical controller designs in which feedback signals are computed directly from measurements by applying proportional, integral, and derivative (PID) gains, the LQG formulation allows the control system designer to directly exploit a linear model for the system dynamics. The controller consists of two portions: a linear observer that is optimized for Gaussian measurement noise and a control law that satisfies a quadratic performance criterion. The observer equation provides an estimate, $\tilde{\vec{x}}_{k+1} = \Phi\tilde{\vec{x}}_k + K_O(\vec{y}_k - C\tilde{\vec{x}}_k)$, of the system state $\vec{x}$ at time-step k+1 given a vector of measurements $\vec{y}$. The matrix Φ characterizes the closed-loop system dynamics, and advances the state estimate $\tilde{\vec{x}}$ based on its previous value. The estimation error, that is, the difference between $\vec{y}$ and the estimated measurements $C\tilde{\vec{x}}_k$, enters via an "observer gain" K_O. In the LQG formulation, K_O and Φ are chosen so that the estimation error is minimized when the uncertainties in $\vec{x}$ and $\vec{y}$ have Gaussian probability distributions.

The feedback inputs $\vec{u}$ are given by the control law

$$\vec{u}_k = K_C\tilde{\vec{x}}_k \quad . \tag{1}$$

Here K_C is a gain matrix that minimizes the expected value of the performance criterion $J = \sum_{k=k_0}^{k_n}(\vec{x}'_k Q_C \vec{x}_k + \vec{u}'_k R_C \vec{u}_k)$ between time-steps k_0 and k_n. Here, the prime ($'$) denotes a vector transpose and the matrices Q_C and R_C are adjusted to preferentially weight the priority in minimizing the system state versus minimizing control effort. In addition to using the optimized gain matrix just described, the control law expressed in Eq. (1) differs from a classical, proportional gain control law in that the gain is applied to the observer's estimate $\tilde{\vec{x}}$ rather than direct measurements of the system.

In this case, the DIII-D VALEN model is used for the controller design, and the methods of casting the VALEN equations in state-space form and reducing the order of the system using balanced realization are followed as in Ref. [10]. LQG controller matrices are then calculated using the reduced system matrices. For the calculations presented here, the controller is untuned, that is, the Q_C and R_C are left as identity matrices.

4. Feedback simulations

Closed-loop eigenvalue calculations with the full-order VALEN model matrices are used to compare the effectiveness of various control algorithm designs in stabilizing the RWM. In addition to the LQG controller described above, a proportional gain control law with an adjustable toroidal phase-shift $\delta\varphi$ is evaluated. For the sake of comparison with the proportional gain controller, an additional, variable phase-shift is applied to the output of the LQG controller as well. Both controllers utilize DIII-D's external control coils and internal, midplane poloidal field sensors, pictured in Fig. 2

The efficacy of using a proportional gain controller was investigated by calculating the closed-loop system eigenvalues for a range of proportional gain and phase-shift settings. The

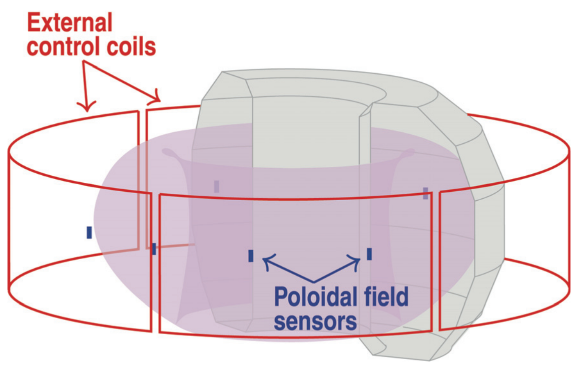

Fig 2. Locations of DIII-D's external, non-axisymmetric control coils (red) and midplane poloidal field sensors (blue).

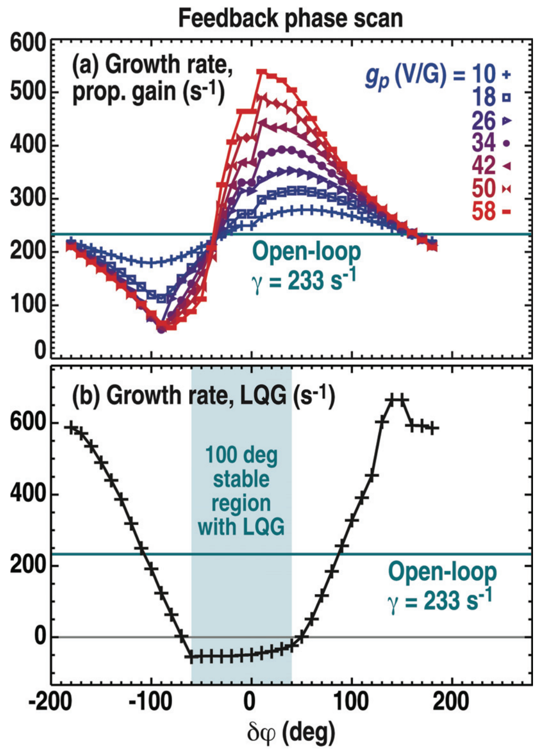

Fig 3. Real parts of closed-loop growth rates for scans of feedback gain and phase angle with a proportional gain controller (a), and for a scan of the feedback phase angle with the LQG controller (b). The horizontal turquoise lines mark the open-loop system growth rate.

maximum real growth rates from these calculations are depicted in Fig. 3(a), as a family of curves that are functions of $\delta\varphi$. As the gain g_p is increased, a local minimum in the growth rate is observed near $\delta\varphi = -90°$ and $g_p = 30$ coil Volts/sensor Gauss. The results for $-90° \leq \delta\varphi \leq 10°$ and $10 \leq g_p \leq 100$ V/G are displayed as a function of proportional gain in Fig. 4. A second local minimum growth rate can be seen near $\delta\varphi = -70°$ and $g_p = 85$ V/G. An extension of this calculation to $g_p = 500$ V/G did not reveal additional minima in the growth rate at any phasing. No combination of proportional gain and phase-shift was found that resulted in closed-loop stability.

An analogous scan of the feedback phase of the LQG controller is shown in Fig. 3(b). Here, a stable system is obtained with no additional phase-shift, $\delta\varphi = 0°$, and stability is maintained inside a 100° window of $\delta\varphi$ settings approximately centred about 0°.

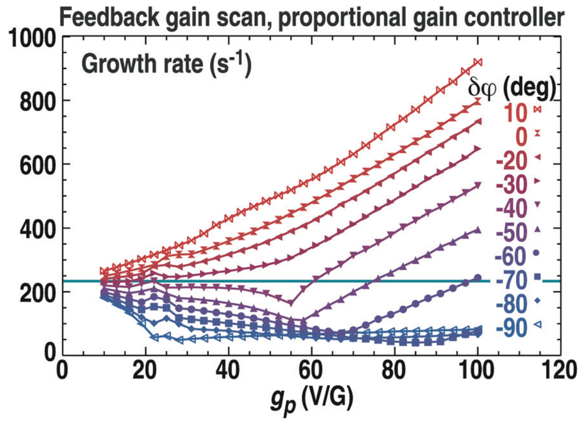

Fig 4. Real parts of the closed-loop growth rate for scans of the feedback gain and phase angle with a proportional gain controller, plotted as a function of the gain. The horizontal turquoise line marks the open-loop system growth rate.

5. Discussion

The eigenvalue calculation results shown in Fig. 3 indicate that the LQG controller formulation is a promising avenue for reliable RWM control with external coils. Consistent with the findings for ITER [10], using an LQG controller enables stabilization of modes that have growth rates that are beyond the reach of proportional gain control. In order to fully assess the usefulness of this technique, the impacts of sensor signal-to-noise ratios, power supply saturation limits, and feedback controller latency must also be characterized. These nonlinear, but experimentally relevant, effects can be investigated using time-domain simulations with the VALEN model. Calculations of this nature are in progress.

This work was supported by the US Department of Energy under DE-FG02-04ER54761, DE-AC05-06OR23100, DE-FG02-06ER84442, DE-AC02-09CH11466, and DE-FC02-04ER54698.

[1] T. Hender, *et al.,* Nuclear Fusion **47**, S128 (2007).
[2] C. Cates, *et al.,* Phys. Plasmas **7**, 3133 (2000).
[3] A. Garofalo, *et al.,* Nucl. Fusion **40**, 1491 (2000).
[4] S.A. Sabbagh, *et al.,* Phys. Rev. Lett. **97**, 045004 (2006).
[5] E.J. Strait, *et al.,* Phys. Plasmas **11**, 2505 (2004).
[6] Y. In, *et al.,* Phys. Plasmas **13**, 062512 (2006).
[7] J.M. Hanson, *et al.,* Phys. Plasmas **15**, 080704 (2008).
[8] J.M. Hanson, *et al.,* Phys. Plasmas **16**, 056112 (2009).
[9] J. Bialek, A.H. Boozer, M.E. Mauel, and G.A. Navratil, Phys. Plasmas **8**, 2170 (2001).
[10] O. Katsuro-Hopkins, J. Bialek, D. Maurer, and G. Navratil, Nucl. Fusion **47**, 1157 (2007).
[11] M. Okabayashi, *et al.,* Nucl. Fusion **49**, 125003 (2009).
[12] A.H. Glasser and M.S. Chance, Bull. Am. Phys. Soc. **42**, 1848 (1997).